Journal Name

Dynamic Article Links ►

Cite this: DOI: 10.1039/c0xx00000x

www.rsc.org/xxxxxx

ARTICLE TYPE

New oxazoline- and thiazoline-containing heteroleptic iridium(III) complexes for highly-efficient phosphorescent organic light-emitting devices (PhOLEDs): colour tuning by varying the electroluminescence bandwidth†

Kai Chao,[a] Kuizhan Shao[a], Tai Peng[b], Dongxia Zhu*[a], Yue Wang[b], Yu Liu*[b], Zhongmin Su[a], Martin R. Bryce*[c]

Two new homologous phosphorescent iridium complexes, bis-(2-phenylpyridine)(2-(2′-hydroxyphenyl)-2-oxazoline)iridium(III) [$(ppy)_2Ir(oz)$] (**1**) and bis-(2-phenylpyridine)(2-(2′-hydroxyphenyl)-2-thiazoline)iridium(III) [$(ppy)_2Ir(thoz)$] (**2**), have been obtained in good yields and characterized by single-crystal X-ray diffraction, cyclic voltammetry, photoluminescence and electroluminescence studies, and by time-dependent density functional theory (TD-DFT) calculations. Using the two complexes, which differ only by the heteroatom (O or S) substitution at the same site in the ancillary ligand, as the emitter, doped in a 4,4′-bis(*N*-carbazolyl)biphenyl (CBP) host, gave phosphorescent organic light-emitting diodes (PhOLEDs) with very efficient green and yellow emission, respectively. The turn-on voltages for both devices are low (3.5-3.7 V). The green-emitting $(ppy)_2Ir(oz)$ –based device has a maximum brightness of 61560 cd m^{-2} (at 16 V); maximum luminance efficiency of 66.2 cd A^{-1}, 17.1% external quantum efficiency, 54 lm W^{-1} power efficiency and CIE coordinates of (0.35, 0.61) at a brightness of 10000 cd m^{-2}. For the yellow-emitting $(ppy)_2Ir(thoz)$-based device with a wide full spectral width at half maximum (FWHM) of 110 nm, the corresponding values are 21350 cd m^{-2} (at 14.5 V); 27.0 cd A^{-1}, 8.5%, 18.0 lm W^{-1} and CIE coordinates of (0.46, 0.50). Colour tuning is primarily a consequence of the significantly wider emission bandwidth of complex **2** compared to complex **1**.

1. Introduction

Organic light emitting diodes (OLEDs) are becoming increasingly successful in new display and lighting technologies.[1] Although OLEDs have reached commercialization, there is still a need for improvements in efficiency, colour purity and stability. Since the pioneering work of Forrest et al.,[1b] enormous experimental and theoretical efforts have focused on the design, synthesis, and characterization of different classes of homoleptic and heteroleptic iridium(III) complexes resulting in improved phosphorescent materials which give increased efficiencies and enhanced brightness, as well as extended operational lifetimes of phosphorescent OLEDs (PhOLEDs).[2] A large number of iridium complexes have been utilized for these purposes, which are mostly based on the cyclometalating (C^N) 2-phenylpyridine (ppy) ligand with an ancillary ligand such as acetylacetonate (acac) or picolinate (pic).[3] Several groups have demonstrated considerable tuning of the phosphorescence wavelengths of the complexes from blue to red by functionalization of the ligands with electron-withdrawing and electron-donating substituents.[4] On the other hand, adjustment of emission colour can also be realized by tuning the emission bandwidth (narrower or wider), which is attractive and important for both fundamental research and practical applications. However, to date this approach has been limited in extent.[5]

In this work, we report the synthesis, structure, electrochemical, photophysical and electroluminescent (EL) properties of two new iridium(III) complexes, namely, bis(2-phenylpyridine)(2-(2′-hydroxyphenyl)-2-oxazoline)iridium(III) (**1**) and bis-(2-phenylpyridine)(2-(2′-hydroxyphenyl)-2-thiazoline)iridium(III) [$(ppy)_2Ir(thoz)$] (**2**). The ancillary N^O oxazoline (oz) and thiazoline (thoz) ligands were chosen as they are readily available and have not been studied previously in this context. We demonstrate that these complexes, which are easily prepared, exhibit emission characteristics which are controlled by the different ancillary ligands. In particular, the two complexes have similar EL peaks at ca. 530 nm for $(ppy)_2Ir(oz)$ **1** and 540 nm for $(ppy)_2Ir(thoz)$ **2**, but they show considerable variation in full width at half maximum (FWHM) values of 70 and 110 nm, respectively. As a result, pure green emission for **1** and yellow emission for **2** with CIE coordinates of (0.35, 0.61) and (0.46, 0.50), respectively, at a brightness of 10000 cd m^{-2}, are achieved in the EL devices based on **1** and **2**, respectively. Both devices show highly efficient EL performance: the green $(ppy)_2Ir(oz)$ **1** device has a maximum brightness of 61560 cd m^{-2} (at 16 V), a maximum luminance efficiency (LE) 66.2 cd A^{-1},17.1 % external quantum efficiency (EQE) and 54 lm W^{-1} for power efficiency (PE). The comparable data for the yellow $(ppy)_2Ir(thoz)$ **2** device

are 21350 cd m^{-2} (at 14.5 V), 27.0 cd A^{-1}, 8.5 % and 18.0 lm W^{-1}, respectively.

Experimental section

Synthesis and characterization

Materials obtained from commercial suppliers were used without further purification unless otherwise stated. All glassware, syringes, magnetic stirring bars, and needles were thoroughly dried in a convection oven. Reactions were monitored using thin layer chromatography (TLC). Commercial TLC plates were used and the spots were visualized under UV light at 254 and 365 nm. 1H NMR spectra were recorded on a Bruker Avance 500 MHz spectrometer with tetramethylsilane as the internal standard at room temperature. Mass spectra were obtained using a Bruker Autoflex Speed MALDI-TOF spectrometer. The chemical structures of the ligands and the corresponding new complexes are shown in **Fig. 1**.

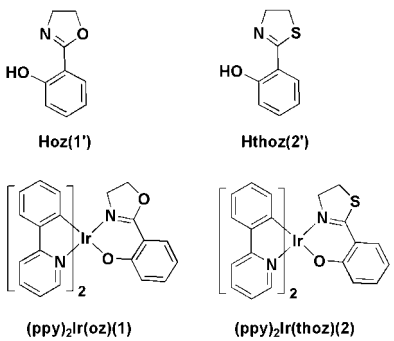

Fig. 1 Chemical structures of the ligands and complexes.

2-(2′-Hydroxyphenyl)-2-oxazoline (Hoz)(1′). A procedure in the literature[6] was applied for this synthesis. MS: *m/z* = 163.08 (M^+). Anal. Calcd. for $C_9H_9NO_2$: C 66.25, H 5.56, N 8.58; Found: C 66.48, H 5.59, N 8.63. ^{1}H NMR ($CDCl_3$, 400 MHz): δ 4.11 (t, 2H, *J* = 9 Hz), 4.41-4.45 (m, 2H), 6.85-6.89 (m, 1H), 7.00-7.02 (m, lH), 7.35-7.38 (m, lH), 7.64-7.66 (m, 1H), 12.18 (s, 1H).

2-(2′-Hydroxyphenyl)-2-thiazoline (Hthoz)(2′). The synthesis of **2′** was similar to that of **1′**. MS: *m/z* = 179.06 (M^+). Anal. Calcd. for C_9H_9NOS: C 60.31, H 5.06, N 7.81; Found: C 60.43, H 5.19, N 7.73. ^{1}H NMR ($CDCl_3$, 400 MHz): δ 3.37 (t, *J* = 8 Hz, 2H), 4.48 (t, *J* = 8 Hz, 2H), 6.86-6.89 (m, 1H), 6.90-7.01 (m, 1H), 7.33-7.36 (m, 1H), 7.41-7.43 (m, 1H), 12.69 (s, 1H).

Bis-(2-phenylpyridine)(2-(2′-hydroxyphenyl)-2-oxazoline)iridium(III) [(ppy)$_2$Ir(oz)] (1).

The complex $[(ppy)_2Ir(\mu\text{-}Cl)]_2$ was synthesized by the standard procedure.[7] A mixture of $[(ppy)_2Ir(\mu\text{-}Cl)]_2$ (0.400 g, 0.330 mmol), Na_2CO_3 (0.349 g, 3.29 mmol), and Hoz (**1′**) (0.150 g, 0.855 mmol) dissolved in 2-ethoxyethanol (30 mL) was stirred under an N_2 atmosphere at 130 °C for 6 h. EtOAc (150 mL) was added after the solution was cooled to RT and washed with water (100 mL) to remove 2-ethoxyethanol. The precipitate was collected by filtration and washed with ethanol (20 mL), followed by diethyl ether (10 mL). Silica gel column purification with *n*-hexane:EtOAc (5:1 v/v) as eluent gave **1** as a yellowish-green powder (0.217 g, 85%). MS: m/z = 663.12 (M+) Anal. Calcd. for $C_{31}H_{24}IrN_3O_2$: C 55.18, H 3.65, N 6.34; Found: C 55.39, H 3.79, N 6.26. ^{1}H NMR ($CDCl_3$, 500 MHz) δ 3.0 (d, *J* = 13 Hz, 1H), 3.52-3.55 (m, 1H), 4.18 (t, *J* = 2Hz, 1H), 4.30 (d, *J* = 1 Hz, 1H), 6.23 (d, *J* = 8 Hz, 1H), 6.33–6.35 (m, 2H), 6.66–6.71 (m, 2H), 6.74 (t, *J* = 8 Hz, 1H), 6.81–6.86 (m, 2H), 7.01–7.12 (m, 1H), 7.12 (d, *J* = 7 Hz, 2H), 7.26-7.58 (m, 2H), 7.61 (d, *J* = 2 Hz, 1H), 7.63-7.66 (m, 1H), 7.68-7.74 (m, 1H), 7.85 (t, *J* = 9 Hz, 2H), 8.38 (d, *J* = 6 Hz, 1H), 8.89 (d, *J* = 7 Hz, 1H).

Bis-(2-phenylpyridine)(2-(2′-hydroxyphenyl)-2-thiazoline)iridium(III)[(ppy)$_2$Ir(thoz)](2). This complex was prepared by analogy with the procedure for **1** using **2′** instead of **1′** to give **2** as a yellow powder (0.388 g, 73%). MS(MALDI-TOF): *m/z* = 678.79 (M^+). Anal. Calcd. for $C_{31}H_{24}IrN_3OS$: C 54.85, H 3.56, N 6.19; Found: C 54.68, H 3.69, N 6.33. ^{1}H NMR ($CDCl_3$, 500 MHz) δ 2.91-2.94 (m, 1H), 3.08 (d, *J* = 10 Hz, 1H), 3.26 (t, *J* = 9 Hz, 1H), 3.94 (d, *J* = 6 Hz, 1H), 6.15 (d, *J* = 8 Hz, 1H), 6.32-6.36 (m, 2H), 6.63 (d, *J* = 8 Hz, 1H), 6.68 (t, *J* = 7 Hz, 1H), 6.72 (t, *J* = 7 Hz, 1H), 6.83 (t, *J* = 8 Hz, 2H), 6.97 (t, *J* = 7 Hz, 1H), 7.09 (t, *J* = 7 Hz, 1H), 7.14-7.26 (m, 1H), 7.43 (d, *J* = 7 Hz, 1H), 7.57 (d, *J* = 8 Hz, 1H), 7.60 (d, *J* = 8 Hz, 1H), 7.64 (t, *J* = 7 Hz, 1H), 7.75 (d, *J* = 7 Hz, 1H), 7.79 (t, *J* = 9 Hz, 1H), 7.88 (d, *J* = 8 Hz, 1H), 8.33 (d, *J* = 6 Hz, 1H), 8.97 (d, *J* = 6 Hz, 1H).

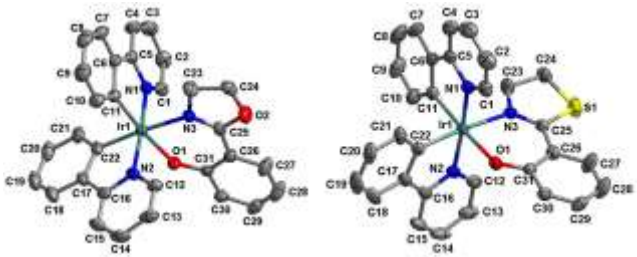

Fig. 2 ORTEP drawings of **1** (left) and **2** (right).

The molecular structures of **1** and **2** were further confirmed by X-ray crystallographic analysis of single crystals obtained by ether diffusion into saturated CH_2Cl_2/CH_3OH (3:1 v/v) solutions. Diffraction data were collected on a Bruker SMART Apex CCD diffractometer using *k*(Mo-Kα) radiation (*k* = 0.71073 Å). Cell refinement and data reduction were made by the SAINT program. The structure was determined using the SHELXTL/PC program. All non-hydrogen atoms were refined anisotropically, whereas hydrogen atoms were placed at the calculated positions and included in the final stage of refinements with fixed parameters. **Fig. 2** shows Oak Ridge thermal ellipsoid plot (ORTEP) drawings of **1** and **2**, and crystallographic data for both complexes have been deposited with the Cambridge Crystallographic Data Centre with CCDC deposition numbers 835020 for **1** and 835019 for **2**. These data can be obtained free of charge from The Cambridge Crystallographic Data Centre via www.ccdc.cam.ac.uk/data_request/cif.

Absorption, photoluminescence (PL) and electrochemical measurements

Absorption spectra were obtained using a Shimadzu UV-2550 UV-vis spectrometer. PL spectra were recorded using a Perkin-Elmer LS-55 fluorescence spectrometer with a Xe arc lamp

excitation source. The PL quantum yields were measured by using quinine sulfate in 1 M sulfuric acid as a standard (Φ = 0.546).[8] All solvents were degassed via three freeze–pump–thaw cycles. Electrochemical measurements were performed in anhydrous CH_2Cl_2 with a BAS 100 W bioanalytical electrochemical work-station, using Pt as the working electrode, platinum wire as the auxiliary electrode, and a porous glass wick (Ag/Ag^+) as the reference electrode. The data was standardized against a ferrocene/ferrocenium couple with a scan rate of 100 mV s^{-1}. The highest occupied molecular orbital (HOMO) and the lowest unoccupied molecular orbital (LUMO) energy levels of the emitting materials were calculated from the cyclic voltammetry (CV) data together with their absorption spectra.

Fabrication of the OLEDs and EL Measurements

The devices were assembled on glass substrates which were precoated with indium tin oxide (ITO) having a sheet resistance of 20 Ω cm^{-2}. The ITO glass was routinely cleaned by ultrasonic treatment in detergent solutions, followed by rinsing with acetone, boiling in isopropanol, and rinsing in methanol and then in de-ionized water. The glass was dried in a vacuum oven between each cleaning step. To reduce the possibility of electrical shorts on the ITO anode and to increase the value of its work function, the ITO substrate was treated using a Plasma Cleaner (PDC-32G-2, 100 W) under an oxygen atmosphere. Prior to the deposition, all the organic materials were purified by sublimation. The organic layers were sequentially deposited onto the substrate at identical pressures of *ca*. 10^{-4} Pa. A very thin layer of LiF was applied to enhance electron injection from the aluminum cathode. The OLEDs consist of a hole-transporting layer (HTL) of 4,4-bis(*N*-(1-naphthyl)-*N*-phenylamino)biphenyl (NPB), a light-emitting layer (EML) of the Ir complexes doped into 4,4′-bis(*N*,*N*-carbazolyl)biphenyl (CBP), an electron-transporting layer (ETL) as well as a hole-blocking layer (HBL) of 1,3,5-tris(*N*-phenylbenzimidazol-2-yl)benzene (TPBI).[9] Except for the phosphors, i.e. $(ppy)_2Ir(oz)$ (**1**) and $(ppy)_2Ir(thoz)$ (**2**), all the organic materials were purchased from Luminescence Technology Corp. or e-Ray Optoelectronics Technology Co. Ltd. and used as received without further purification.

The basic OLED configuration is ITO/NPB/EML/TPBI/LiF/Al. The EML is 8 wt% $(ppy)_2Iroz$ or $(ppy)_2Irthoz$: CBP. A shadow mask with 2×3 mm^2 openings was used to define the cathodes. The EL spectra, brightness, CIE coordinates and the current–brightness–voltage characteristics of the devices were measured with a rapid-scan system using a spectrophotometer (PR-650, Photo Research) and a computer-controlled, programmable direct-current (DC) source (Keithley 2400). Luminance–voltage and current–voltage characteristics were measured at room temperature under an ambient atmosphere.

Results and discussions

Photophysical and electrochemical properties

The UV/vis absorption spectra of the complexes $(ppy)_2Ir(oz)$ (**1**) and $(ppy)_2Ir(thoz)$ (**2**) in degassed solution (CH_2Cl_2) and the PL emission spectra in degassed CH_2Cl_2 and in solid neat film are shown in **Fig. 3** and the corresponding data are summarized in Table 1. The absorption bands of both complexes below 350 nm, with the peaks at 249 and 340_{sh} nm for **1** and 243 and 330_{sh} nm for **2**, can be assigned to spin-allowed $^1\pi$–π^* transitions on the cyclometalated ligands. The weaker and broad absorption bands extending from 350 nm to the visible region, 377_{sh} and 443_{sh} nm for **1** and 383_{sh} and 445_{sh} nm for **2**, are primarily due to the spin-allowed metal-to-ligand-charge-transfer (^{1}MLCT) transitions, ^{1}LLCT (ligand-to-ligand charge-transfer), ^{3}MLCT, ^{3}LLCT, and ligand-centered (LC) $^3\pi$-π^* transitions. As the presence of the heavy iridium center results in a strong spin-orbit coupling, the spin-forbidden ^{3}MLCT, ^{3}LLCT, and LC $^3\pi$-π^* transitions become partially allowed and gain considerable intensity by mixing with the ^{1}MLCT transitions.[10d,e] The emission maxima of **1** and **2** in dichloromethane solution are at 527 nm and 542 nm, respectively. These peaks are slightly red-shifted in solid films to 530 nm and 558 nm, respectively. Here, it is noticeable that the PL spectra of $(ppy)_2Ir(thoz)$ (**2**) exhibits a much broader bandwidth towards the long-wavelength region than $(ppy)_2Ir(oz)$ (**1**), resulting in differences in the emission colours, which are green and yellow for **1** and **2**, respectively, although $(ppy)_2Ir(thoz)$ **2** does not display a typical emission peak (*ca.* 542 nm) for yellow light. Broadened emission bands have been ascribed to interligand energy transfer processes.[5b] The solution luminescence quantum yield (Φ_L) was measured to be 0.55 for **1** and 0.27 for **2**, respectively, by using the method of Demas and Crosby.[8a]

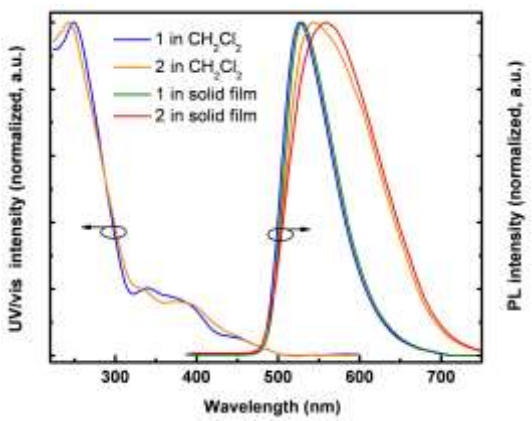

Fig. 3 UV-Vis absorption and PL emission spectra of complexes (**1**) and (**2**) in degassed solution (CH_2Cl_2) and in solid film at room temperature.

Table 1. Photophysical and electrochemical data for complexes **1** and **2**.

Complex	Abs λ_{max}[a] (nm)	PL λ_{max}[a] (nm)	PL λ_{max}[b] (nm)	Φ_{PL}[a]	Lifetime τ[c] (μs)	K_r ($\times 10^6$ s^{-1})[d]	K_{nr} ($\times 10^6$ s^{-1})	HOMO (eV)	LUMO (eV)	E_{gap} (eV)
1	249, 340_{sh}, 377_{sh}, 443_{sh}	527	530	0.55	0.341	1.61	1.32	–4.75	–2.30	2.45
2	243, 330_{sh}, 383_{sh}, 445_{sh}	542	558	0.27	0.485	0.56	1.51	–4.80	–2.45	2.35

[a] Measured in CH_2Cl_2 (1.0×10^{-5} M). [b] Measured in the film state. [c] Lifetime data in degassed CH_2Cl_2 solution: excitation wavelength 285 nm. [d] k_r and k_{nr} in solution were calculated according to the equations: $k_r = \Phi/\tau$ and $k_{nr} = (1-\Phi)/\tau$.

The excited state lifetimes of complexes **1** and **2** in degassed CH_2Cl_2 solution are shown in Table 1. They are relatively long – on the order of microseconds – and are consistent with a mixture of LC $^3\pi$-π^* and ^{3}MLCT character for the emissive excited

states.[10f] The radiative k_r and non radiative decay rates k_{nr} were calculated using the equations $k_r = \Phi/\tau$ and $k_{nr} = (1-\Phi)/\tau$ from the quantum yields Φ and the lifetime τ values.[10g,h] The higher quantum yields of **1** can be attributed to its increased radiative rate which is significantly greater than that of **2**.[2b]

The electrochemical properties of **1** and **2** were studied in solution by cyclic voltammetry (CV) measurements using ferrocene as the internal standard. Their electrochemical data are summarized in Table 1 and CVs are shown in the Supporting Information. Both complexes display one reversible oxidation wave; no reduction waves were detected within the electrochemical window of dichloromethane. The HOMO and the LUMO energy levels were calculated from the onset potentials for oxidation together with their absorption spectra. The HOMO energy levels vary from –4.75 eV for **1** to –4.80 eV for **2**, and the corresponding LUMO levels are –2.30 eV and –2.45 eV, respectively. Clearly, the HOMO energy levels of complexes **1** and **2** are little affected by the oxazoline or thiazoline frameworks, whereas their LUMO levels change relatively significantly due to the different ancillary ligands.

Theoretical Calculations

To probe the structure–property relationships of the complexes at the molecular level, their geometrical and electronic properties were studied using time-dependent density functional theory (TD-DFT). The features of the frontier orbitals mainly involved in the electronic transitions are depicted in **Fig. 4**, while the descriptions and the energy gap of each transition are listed in Table 2.

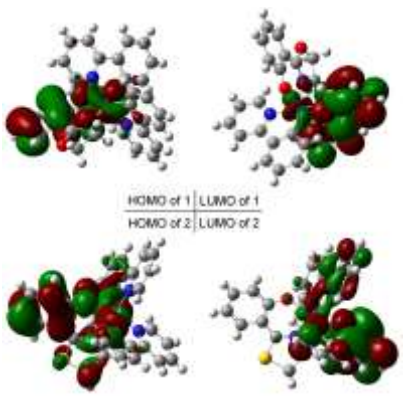

Fig. 4 The contour plots of the HOMOs and LUMOs of complexes $(ppy)_2Ir(oz)$ (**1**) and $(ppy)_2Ir(thoz)$ (**2**) from DFT calculations.

Both complexes **1** and **2** reveal a similar frontier orbital configuration. Their HOMOs are mainly spread over the Ir atom and the phenolate ring of the ancillary ligand, which is less affected by the variations in the ancillary ligand structure in the homologous complexes. The LUMOs are localized mostly on the neutral pyridine ring of a ppy ligand. From the calculations, the energy gap of **1** is larger than **2**. This result may be rationalized by the fact that the sulfur atom in the thiazoline moiety in **2** is more polarizable than the equivalent oxygen atom in **1**, resulting in an increase of the conjugative effect in **2** and hence a smaller energy gap for **2**. The calculated energy gaps follow the order: **1** (3.22 eV) > **2** (2.83 eV), which is consistent with the trends in their PL and EL spectra, and the electrochemical properties from CV measurements.

Table 2. TD-DFT Calculation Results for Complexes **1** and **2**.

	Transition energy	Participating MO	Transition character[a]	Energy gap (eV)
1	438.6 nm	HOMO→ LUMO HOMO→ LUMO+1	$ML_ACT+L_AC+L_CL_ACT$ + ML_BCT	3.22
	365.2 nm	HOMO→ LUMO+4	ML_CCT+L_CC	
	272.3 nm	HOMO→ LUMO+2 HOMO→LUMO+3	$ML_{AB}CT+L_AL_BCT+L_CL_ACT$	
2	458.5 nm	HOMO→ LUMO+2 HOMO→ LUMO+5	L_CC	2.83
	330.7 nm	HOMO→ LUMO HOMO→ LUMO+1 HOMO→ LUMO+2 HOMO→ LUMO+3 HOMO→ LUMO+4 HOMO→ LUMO+5	$ML_ACT+L_AL_BCT+ML_CCT+L_AL_CCT+L_CC$	

a) Excitation energies calculated for the triplet states; b) Ligand notation: A, B = 2-phenylpyridine; C = 2-(2′-Hydroxyphenyl)-2-oxazoline or 2-(2′-Hydroxyphenyl)-2-thiazoline.

To assist in assigning the nature of the excited states involved in the experimental absorption spectra, the singlet excited states were obtained based on TD-DFT calculations. The transition character, orbital distributions and the simulated UV-Vis absorption spectra of both complexes, are summarized in Table 2, Tables S1-S2 and Figures S2-S3 (See ESI). Based on TD-DFT results, the high-energy absorption bands (λ_{abs} <400 nm) are composed of MLCT in combination with π–π* transitions (ILCT and LLCT) in character. However, the transition characters from the absorption bands from 400 nm extending to the visible region for **1** and **2** are different. For **1**, the calculated absorption maximum at 438.6 nm is mainly attributed to MLCT and LLCT characters, while predominant LC character is observed for complex **2** according to the theoretical results. The difference between the excited states of complexes **1** and **2**, such as much more MLCT characters in the excited state and relatively wide energy gap (see Table 2) for **1** relate to the higher radiative decay and lower non-radiative decay.[10f, 2b] As a result, complex **1** is expected to exhibit shorter excited lifetime and higher quantum efficiency compared with **2**, which is consistent with the experimental data.

Electrophosphorescent properties

The PhOLED configuration is ITO/NPB/EML/TPBI/LiF/Al. The EML is 8 wt% $(ppy)_2Ir(oz)$ (**1**) (device I) or $(ppy)_2Ir(thoz)$ (**2**) (device II):CBP. The devices I and II exhibit bright green and yellow emission, respectively, independent of the applied voltages in the range of 3 V to 16 V. The normalized EL spectra of both devices at a brightness of 10000 cd m^{-2} are shown in Fig. 5. Devices I and II have a similar EL emission peak at around λ_{max} 530–540 nm, but show a significant difference in the emission bandwidth. Device I using $(ppy)_2Ir(oz)$ (**1**) as the emitter displays a narrow spectral profile with a FWHM of ~70 nm and green emission with CIE coordinates of (0.35, 0.61). In comparison, device II based on $(ppy)_2Ir(thoz)$ (**2**), shows a considerably broadened EL spectral bandwidth with FWHM of ~110 nm leading to yellow emission with CIE coordinates of

(0.46, 0.50). The EL spectra of devices I and II are consistent with the PL spectra of both complexes (Fig. 3). The fact that no host emission is observed in the EL spectra establishes that complete energy transfer occurs from CBP to the Ir complex, as was expected for a doping concentration of 8 wt%, in which the emission occurs solely from the Ir complexes.

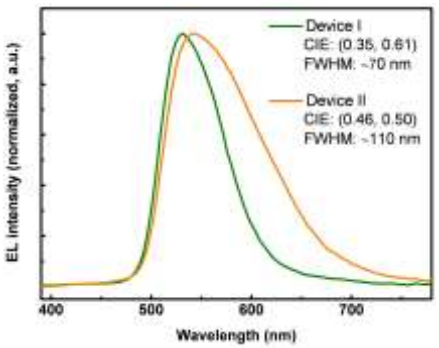

Fig. 5 EL spectra of devices I and II at a brightness of 10000 cd m^{-2}.

Fig. 6 shows the current-density–voltage–brightness characteristics of the devices I and II. In addition, both devices have high EL efficiencies as shown in **Fig. 7**. Devices I and II exhibited low turn-on voltages (recorded at 1 cd m^{-2}) of 3.5 V and 3.7 V, respectively. The EL intensities of both devices show a rapid rise after the onset voltage and the corresponding peak radiances were obtained at 16 V for device I (61560 cd m^{-2}) and at 14.5 V for device II (21350 cd m^{-2}). The driving voltages of device I and II required to achieve 100 and 1000 cd m^{-2}, 20 and 100 mA cm^{-2}, are 5.7, 7.8, 10.4, 12.6 V and 6.6, 8.8, 10.4, 12.5 V, respectively. These comparatively low operating voltages suggest that an effective charge transport exists throughout the devices. As a result, the maximum LE, EQE and PE values can reach very high levels of 66.2 cd A^{-1}, 17.2 % and 54.0 lm W^{-1}, respectively, for device I with green emission, and 27.0 cd A^{-1}, 8.5 %, 18.0 lm W^{-1} for device II with yellow emission.

Both devices (I and II) present high EL efficiencies, which are competitive with the highest-efficiency literature values utilizing comparable simple device architectures.[11] For example, during the preparation of this manuscript, Tan et al, reported a new heteroleptic Ir phosphor with green emission: iridium(III) bis[2-(1-phenoxy-4-phenyl)-5-methylpyridine](acetylacetonate) with maximum values of 102525 cd m^{-2} (at 15 V); 84.6 cd A^{-1}, EQE 24.5%, 77.6 lm W^{-1}, CIE (0.26, 0.63).[11a] We emphasise that devices I and II achieve highly efficient green and yellow emission *by utilizing a simple device structure*, making both complexes **1** and **2** good candidates for display and illumination applications. Moreover, the device using $(ppy)_2Ir(thoz)$ phosphor **2** displays yellow EL with an unusually wide FWHM of ~110 nm, which does not rely on the presence of excimer emission. Indeed, to our knowledge, the FWHM of device II is the highest value for a yellow OLED without excimer emission to have been reported in the literature.[12] The efficiency data for device II compare favourably with the best yellow phosphors in similar device architectures.[13] For example, iridium(III) bis[2-(2-naphthyl)pyridine](acetylacetonate) $[Ir(npy)_2(acac)]$ 34 cd A^{-1}, 22 lm W^{-1}, EQE 11%, CIE 0.45, 0.54;[13a] iridium(III) bis[2-(3-diphenylphosphanylpyridine)](acetylacetonate) 51.6 cd A^{-1}, 27 lm W^{-1}, EQE 14.5%, CIE 0.44, 0.53.[13b]

Such wide-FWHM yellow emission could significantly increase the spectral coverage of white OLEDs (WOLEDs) especially where white light is attained *via* combination of blue and complementary yellow (BY) emissions, resulting in a high Color Rendering Index (CRI).[14] In addition, it is important to note that tuning of the CIE coordinates through adjusting the emission bandwidth has been realized by simply selecting different ancillary ligands in complexes **1** and **2**.

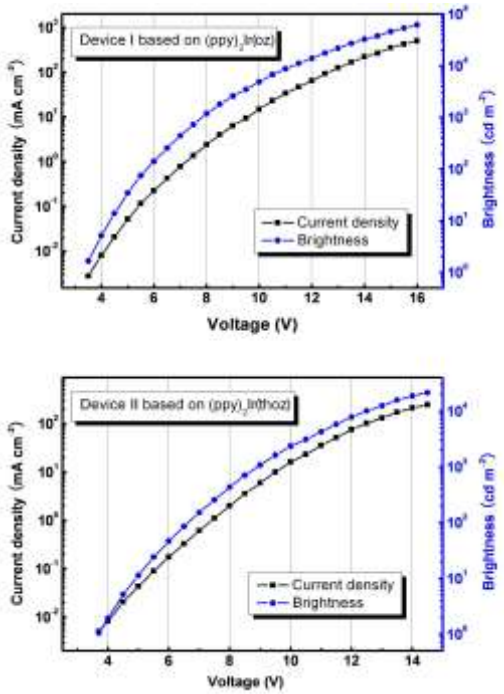

Fig. 6 Current-density–brightness–driving voltage curves of device I (top) and II (bottom).

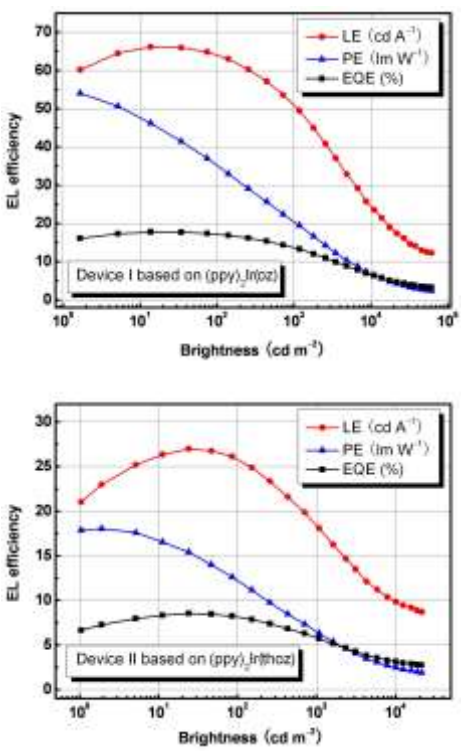

Fig. 7 LE-, PE- and EQE–brightness characteristics of device I (top) and II (bottom).

Conclusions

The synthesis of electrophosphorescent iridium complexes from new cyclometalating ligands (C^N) is not always feasible because the traditional chloride-bridged iridium dimer intermediate, $[(C\hat{}N)_2Ir(\mu\text{-}Cl)]_2$, may be difficult to prepare for steric and/or electronic reasons.[15] We have shown that the strategy outlined above, using a readily-available dimer intermediate (i.e. $[(ppy)_2Ir(\mu\text{-}Cl)]_2$) and new ancillary ligands, is a straightforward, efficient and competitive approach to colour tuning of PhOLEDs.[4] We have designed, synthesized and characterized two novel phosphorescent iridium complexes, namely $(ppy)_2Ir(oz)$ **1** and $(ppy)_2Ir(thoz)$ **2**, which have a different ancillary oxazoline (oz) or thiazoline (thoz) ligand, while retaining the cyclometalated ppy ligands. PhOLEDs based on these complexes exhibit high EL performances including peak efficiency values of 66.2 cd A^{-1}, 17.1% and 54 lm W^{-1} for the $(ppy)_2Ir(oz)$-based device I, and 27.0 cd A^{-1}, 8.5% and 18.0 lm W^{-1} for the $(ppy)_2Ir(thoz)$-based device II. Furthermore, devices I and II show different emission colours of green and yellow due to significant variation in their FWHM values of 70 and 110 nm, respectively, although they have similar EL emission peaks of 530-540 nm. The effective tuning of EL colour through adjusting the emission bandwidth is a strategy that has previously received only limited attention.[5] In addition, due to the wide FWHM of $(ppy)_2Ir(thoz)$ (**2**) being a desirable spectral property, further studies will aim at fabricating WOLEDs possessing a high colour rendering index (CRI) based on this yellow emitter.

X-Ray Crystallography

Crystallographic data (excluding structure factors) have been deposited with the Cambridge Crystallographic Data Centre as supplementary publication numbers 835020 (complex **1**), 835019 (complex **2**). Copies of the data can be obtained free of charge from www.ccdc.cam.ac.uk/conts/retrieving.html or on application to The Director, Cambridge Crystallographic Data Centre (CCDC), 12 Union Road, Cambridge CB2 1EZ, UK. E-mail: deposit@ccdc.cam.ac.uk; www.ccdc.cam.ac.uk.

Acknowlegements

The work in China was funded by NSFC (51203017 and 21303012), the Science and Technology Development Planning of Jilin Province (20100540). The work in Durham was funded by EPSRC.

Notes and references

[a] *Institute of Functional Material Chemistry, Faculty of Chemistry, Northeast Normal University, Renmin Road 5268, Changchun 130024 P.R. China;*
E-mail:zhudx047@nenu.edu.cn
[b] *State Key Laboratory of Supramolecular Structure and Materials, Jilin University, Changchun 130012, People's Republic of China;*
E-mail: yuliu@jlu.edu.cn
[c] *Department of Chemistry, Durham University, Durham, DH1 3LE, UK*
E-mail: m.r.bryce@durham.ac.uk

† Electronic supplementary information (ESI) available: Experimental schemes for the complexes, cyclic voltammograms and procedures for the DFT calculations, calculated energy levels and orbital compositions, simulated absorption spectra.

1 (a) R. H. Friend, R. W. Gymer, A. B. Holmes, J. H. Burroughes, R. N. Marks, C. Taliani, D. D. C. Bradley, D. A. Dos Santos, J. L. Brédas, M. Lögdlund, W. R. Salaneck, *Nature*, 1999, **397**, 121; (b) M. A. Baldo, M. E. Thompson, S. R. Forrest, *Nature*, 2000, **403**, 750; (c) G. J. Zhou, W. Y. Wong, X. L. Yang, *Chem.-Asian J*., 2011, **6** , 1706; (d) J. Ye, C. J. Zheng, X. M. Ou, X. H. Zhang, M. K. Fung, C. S. Lee, *Adv. Mater*., 2012 , **24** , 3410; (e) L. X. Xiao, Z. J. Chen, B. Qu, J. X. Luo, S. Kong, Q. H. Gong, J. J. Kido, *Adv. Mater*., 2011 , **23** , 926; (f) B. H. Zhang, G. P. Tan, C. S. Lam, B. Yao, C. L. Ho, L. H. Liu, Z. Y. Xie , W. Y. Wong, J. Q. Ding, L. X. Wang, *Adv. Mater*., 2012, **24**, 1873; (g) Y. L. Chang, B. A. Kamino, Z. Wang, M. G. Helander, Y. Rao, L. Chai, S. Wang, T. P. Bender, Z. H. Lu, *Adv. Funct. Mater*., 2013, **23**, 3204.

2 (a) Y. You, S. Y. Park, *J. Am. Chem. Soc*.**,** 2005, **127**, 12438; (b) J. Li, P. I. Djurovich, B. D. Alleyne, M. Yousufuddin, N. N. Ho, J. C. Thomas, J. C. Peters, R. Bau, M. E. Thompson, *Inorg. Chem.*, 2005, **44**, 1713; (c) S. Lamansky, P. Djurovich, D. Murphy, F. Abdel-Razzaq, H.-E. Lee, C. Adachi, P. E. Burrows, S. R. Forrest, M. E. Thompson, *J. Am. Chem. Soc*., 2001, **123**, 4304; (d) E. Holder, B. M. W. Langeveld, U. S. Schubert, *Adv. Mater*., 2005, **17**, 1109; (e) R. Ragni, E. A. Plummer, K. Brunner, J. W. Hofstraat, F. Babudri, G. M. Farinola, F. Naso, L. De Cola, *J. Mater. Chem.*, 2006, **16**, 1161; (e) Y. You and S. Y. Park, *Dalton Trans*. 2009, 1267; (f) H. A. Al-Attar, G. C. Griffiths, T. N. Moore, M. Tavasli, M. A. Fox, M. R. Bryce and A. P. Monkman, *Adv. Funct. Mater*. 2011, **21**, 2376.

3 (a) M. K. Nazeeruddin, R. Humphry-Baker, D. Berner, S. Rivier, L. Zuppiroli, M. Graetzel, *J. Am. Chem. Soc*., 2003, **125**, 8790; (b) Y. Sun, N. C. Giebink, H. Kanno, B. Ma, M. E. Thompson, S. R. Forrest, *Nature*, 2006, **440**, 908; (c) S. Lamansky, P. Djurovich, D. Murphy, F. Abdel-Razzaq, R. Kwong, I. Tsyba, M. Bortz, B. Mui, R. Bau, M. E. Thompson, *Inorg. Chem.*, 2001, **40**, 1704; (d) M. S. Lowry, W. R. Hudson, R. A. Pascal Jr., S. Bernhard, *J. Am. Chem. Soc.*, 2004, **126**, 14129.

4 (a) P. Coppo, E. A. Plummer, L. De Cola, *Chem. Commun.*, 2004, 1774; (b) T. Sajoto, P. I. Djurovich, A. Tamayo, M. Yousufuddin, R. Bau, M. E. Thompson, R. J. Holmes, S. R. Forrest, *Inorg. Chem.*, 2005, **44**, 7992; (c) Y. You and S. Y. Park, *J. Am. Chem. Soc.*, 2005, **127**, 12438. (d) G. J. Zhou, C. L. Ho, W. Y. Wong, Q. Wang, D. G. Ma, L. X. Wang, Z. Y. Lin, T. B. Marder and A. Beeby, *Adv. Funct. Mater*., 2008, **18**, 499.

5 H. J. Bolink, E. Coronado, S. G. Santamaria, M. Sessolo, N. Evans, C. Klein, E. Baranoff, K. Kalyanasundaram, M. Graetzel, M. K. Nazeeruddin, *Chem. Commun*., 2007, 3276. E. Baranoff, I. Jung, R. Scopelliti, E. Solari, M. Graetzel, Md. K. Nazeeruddin, *Dalton Trans*., 2011, **40**, 6860.

6 H. R. Hoveyda, V. Karunaratne, S. J. Rettig, C. Orvig, *Inorg. Chem.*, 1992, **31**, 5408.

7 S. Sprouse, K. A. King, P. J. Spellane, R. J. Watts, *J. Am. Chem. Soc*., 1984, **106**, 6647.

8 (a) J. N. Demas, G. A. Crosby, *J. Phys. Chem.*, 1971, **75**, 991. (b) C.-H. Chang, K.-C. Tien, C.-C. Chen, M.-S. Lin, H.-C. Cheng, S.-H. Liu, C.-C. Wu, J.-Y. Hong, Y.-C. Chiu, Y. Chi, *Org. Electron*., 2011, **11**, 412.

9 (a) K. R. J. Thomas, J. T. Lin, Y.-T. Tao, C.-W. Ko, *J. Am. Chem. Soc*., 2001, **123**, 9404; (b) B. W. D'Andrade, S. R. Forrest, *Adv. Mater*., 2004, **16** 1585.

10 (a) K. A. King, P. J. Spellane, R. J. Watts, *J. Am. Chem. Soc.*, 1985, **107**, 1431; (b) K. Dedeian, P. I. Djurovich, F. O. Garces, G. Carlson, R. J. Watts, *Inorg. Chem*., 1991, **30**, 1685; (c) S. Lamansky, P. Djurovich, D. Murphy, F. Abdel-Razzaq, H. Lee, C. Adachi, P. E. Burrows, S. R. Forrest, M. E. Thompson, *J. Am. Chem. Soc.*, 2001, **123**, 4304; (d) S. Sprouse, K. A. King, P. J. Spellane, R. J. Watts, *J. Am. Chem. Soc.*, 1984, **106**, 6647; (e) M. G. Colombo, T. C. Brunold, T. Riedener, H. U. Güdel, M. Förtsch, H. B. Bürgi, *Inorg. Chem*., 1994, **33**, 545; (f) K. A. King, R. J. Watts, *J. Am. Chem. Soc*., 1987, **109**, 1589; (g) J. V. Caspar, T. J. Meyer, *J. Phys. Chem.*, 1983, **83**, 952; (h) C. Dragonetti, L. Falciola, P. Mussini, S. Righetto, D. Roberto, R. Ugo, A. Valore, *Inorg. Chem*., 2007, **46**, 8533.

11 (a) G. Tan, S. Chen, N. Sun, Y. Li, D. Fortin, W.-Y. Wong, H.-S. Kwok, D. Ma, H. Wu, L. Wang, P. Harvey, *J. Mater. Chem. C*, 2013, **1**, 808. Improvements in the performance of $Ir(ppy)_3$ or $(ppy)_2Ir(acac)$-doped devices have been achieved by modification of the device structures (e.g., employing a *p*-*i*-*n* structure or utilizing a more efficient exciton-block layer, a higher-mobility electron-transport material or a host material with superior charge mobility, etc.). For examples, see: (a) M. Ikai, S. Tokito, Y. Sakamoto, T. Suzuki, Y. Taga, *Appl. Phys. Lett.*, 2001, **79**, 156; (b) G. He, M. Pfeiffer, K. Leo, M. Hofmann, J. Birnstock, R. Pudzich, J. Salbeck, *Appl. Phys. Lett.*, 2004, **85**, 3911; (c) S.-J. Su, T. Chiba, T. Takeda, J. Kido, *Adv. Mater.*, 2008, **20**, 2125; (d) Y. Z. Li, W. J. Xu, G. Z. Ran, G. G. Qin, *Appl. Phys. Lett.*, 2009, **95**, 033307; (e) Y. Tao, Q. Wang, C. Yang, C. Zhong, K. Zhang, J. Qin, D. Ma, *Adv. Funct. Mater.*, 2010, **20**, 304; (f) Y. Tao, Q. Wang, C. Yang, C. Chong, J. Qin, D. Ma, *Adv. Funct. Mater.*, 2010, **20**, 2923.

12 T. Tsuzuki, N. Shirasawa, T. Suzuki, S. Tokito, *Adv. Mater.*, 2003, **15**, 1455; (b) B.-P. Yan, C. C. C. Cheung, S. C. F. Kui, V. A. L. Roy, C.-M. Che, S.-J. Xu, *Appl. Phys. Lett.*, 2007, **91**, 063508; (c) X.-M. Yu, G.-J. Zhou, C.-S. Lam, W.-Y. Wong, X.-L. Zhu, J.-X. Sun, M. Wong, H.-S. Kwok, *J. Organomet. Chem.*, 2008, **693**, 1518; (d) C.-L. Ho, W.-Y. Wong, G.-J. Zhou, B. Yao, Z. Xie, L. Wang, *Adv. Funct. Mater.*, 2007, **17**, 2925; (e) J. H. Yao, C. Zhen, K. P. Loh, Z.-K. Chen, *Tetrahedron*, 2008, **64**, 10814. (f) W.-S. Huang, J. T. Lin, C.-H. Chien, Y.-T. Tao, S.-S. Sun, Y.-S. Wen, *Chem. Mater.*, 2004, **16**, 2480; (g) I. R. Laskar, S.-F. Hsu, T.-M. Chen, *Polyhedron*, 2005, **24**, 881; (h) Y. Tao, Q. Wang, C. Yang, K. Zhang, Q. Wang, T. Zhou, J. Qin, D. Ma, *J. Mater. Chem.*, 2008, **18**, 4091; (i) M. Li, W.-H. Chen, M.-T. Lin, M. A. Omary, N. D. Shepherd, *Org. Electron.*, 2009, **10**, 863.

13 (a) S. L. Lai, S. L. Tao, M. Y. Chan, M. F. Lo, T. W. Ng, S. T. Lee, W. M. Zhao, C. S. Lee, *J. Mater. Chem.*, 2011, **21**, 4983: (b) L. Deng, T. Zhang, R. Wang, J. Li, *J. Mater. Chem.*, 2012, **22**, 15910.

14 C. H. Chang, C. C. Chen, C. C. Wu, S. Y. Chang, J. Y. Hung, Y. Chi, *Org. Electronics*, 2010, **11**, 266.

15 Y. Zheng, A. S. Batsanov, M. R. Bryce, *Inorg. Chem*, 2010, **50**, 3354.